



# CHORUS

This is the accepted manuscript made available via CHORUS. The article has been published as:

## Shaping attosecond pulses by controlling the minima in high-order harmonic generation through alignment of CO<sub>2</sub> molecules

Cheng Jin, Su-Ju Wang, Xi Zhao, Song-Feng Zhao, and C. D. Lin

Phys. Rev. A **101**, 013429 — Published 23 January 2020

DOI: [10.1103/PhysRevA.101.013429](https://doi.org/10.1103/PhysRevA.101.013429)

# Shaping attosecond pulses by controlling the minima in high harmonic generation through alignment of CO<sub>2</sub> molecules

Cheng Jin,<sup>1,2,\*</sup> Su-Ju Wang,<sup>3</sup> Xi Zhao,<sup>3</sup> Song-Feng Zhao,<sup>4</sup> and C. D. Lin<sup>3</sup>

<sup>1</sup>*Department of Applied Physics, Nanjing University of Science and Technology, Nanjing 210094, China*

<sup>2</sup>*State Key Laboratory of Transient Optics and Photonics,  
Xi'an Institute of Optics and Precision Mechanics,  
Chinese Academy of Sciences, Xi'an 710119, China*

<sup>3</sup>*J. R. Macdonald Laboratory, Department of Physics,  
Kansas State University, Manhattan, Kansas 66506, USA*

<sup>4</sup>*Key Laboratory of Atomic and Molecular Physics and Functional Materials of Gansu Province,  
College of Physics and Electronic Engineering, Northwest Normal University, Lanzhou 730070, China*

We report a simple method for generating shaped attosecond pulses by using CO<sub>2</sub> molecule. Unlike most other molecules, owing to its unique energy and angle dependence and the presence of deep minima in the photoionization transition dipole moment, the shape of harmonic spectra, especially the position and depth of minima, can be readily controlled by tuning the degree of alignment. The sensitive alignment dependence of the minima is due to the coherent interference of laser-induced dipole from each molecule when CO<sub>2</sub> molecules are moderately aligned, but not when they are well-aligned or when they are isotropically distributed. Such a sensitivity offers a simple route for controlling the spectral amplitude and phase of the generated harmonics and thus shaping the generated attosecond pulses; for example, producing structured attosecond pulses by splitting a single burst into two. We illustrate how such pulses are generated and how to characterize them. This method offers a simple way to shape attosecond pulses at the generation step. It can be easily implemented experimentally to generate attosecond pulses with strong phase variations for unique applications.

## I. INTRODUCTION

In the past decades, high harmonic generation (HHG) resulting from the interaction of an intense infrared laser pulse with atoms and molecules has been widely studied [1–6]. Typically, harmonic signals exhibit a fast drop in intensity in the first few orders, then followed by a long plateau region where the intensity of each order remains nearly the same until the cutoff, beyond which harmonics are continuous. Since harmonics are coherent, by synthesizing discrete plateau harmonics, an attosecond pulse train (APT) can be generated [7]. In the time domain, an APT appears as a train of bursts, each of which is of attoseconds duration with a well-behaved shape. Similarly, once the continuous harmonics are synthesized, in the time domain it would appear as an isolated attosecond pulse (IAP), with a well-behaved pulse envelope [8]. IAPs and APTs generated in atomic gas targets have been widely used in numerous attosecond experiments [9, 10] in the past decade.

Harmonics generated from an atom or molecule can be understood qualitatively with the three-step model: ionization, propagation, and recombination [11, 12]. This model has been extended in the quantitative rescattering (QRS) theory [13–15] where the single-atom induced dipole can be expressed as a product of the complex returning electron wave packet  $W(\omega)$  and the complex photo-recombination (PR) transition dipole  $d(\omega)$ , where  $\omega$  is

the photon energy. Here  $d(\omega)$  is the complex conjugate of photoionization (PI) transition dipole which is a property of the atom, and  $W(\omega)$  is the property of the laser pulse. Thus, according to the QRS theory, a minimum in  $|d(\omega)|^2$  would appear as a minimum in the harmonic spectrum. Changing the laser intensity or wavelength can only modify the smooth wave packet but not the position of minimum in the harmonic spectra. This model has been well-established for the harmonic spectra generated at the single-atom level. However, experimentally the observed harmonic spectra are through the coherent buildup of harmonics from multiple atoms in the gas medium, then the position of minimum observed in the harmonic spectra could be influenced by phase-matching conditions, especially at high laser intensities where the medium is modified by the laser. Ar, one of atomic targets, has been most extensively investigated, see e.g., Refs. [16–23].

Harmonic spectra from molecules have also been extensively studied in the past two decades and the minima in the spectra have been of great interest. For each fixed-in-space molecule, the QRS theory also applies such that minimum in the transition dipole moment would lead to minimum in the harmonic spectra. Since molecules in the gas medium are randomly distributed or partially oriented, the generated harmonic spectra should be averaged over the angular distribution of molecules. In addition, in molecules, sub-shell binding energies are not well-separated, thus harmonics can be generated from electrons in the highest occupied molecular orbital (HOMO) as well as from those in the inner-shell orbitals (HOMO-1, HOMO-2, ..., and so on). The contribution to the har-

---

\*Corresponding author. E-mail: cjin@njjust.edu.cn

monics from each subshell should be added coherently. At lower driving laser intensities, the harmonics are generated from the HOMO only. According to the QRS theory, the position of the minimum is independent of either the laser intensity or the wavelength. At higher driving laser intensities, electrons from inner orbitals may also contribute to the harmonics and the position of minimum would then depend upon the laser intensity. Both types of minima have been investigated extensively in the past decades, and the QRS theory has been able to reproduce these measurements in general [13–15]. In particular, CO<sub>2</sub> is one of the most popularly studied molecules, for example, Refs. [24–45].

In spite of the extensive literature on HHG from CO<sub>2</sub> molecules, for years there exists a well-known puzzle between the experiments of *Vozzi et al.* [35] and *Rupenyan et al.* [38]. They reported harmonic spectra for aligned CO<sub>2</sub> molecules with the degree of alignment  $\langle \cos^2 \theta \rangle$  near 0.6, where  $\theta$  is the angle between the molecular axis and laser polarization. In *Vozzi et al.* [35] a sharp minimum was observed at 60 eV, yet in *Rupenyan et al.* [38] a minimum was reported at 47 eV. In a theoretical simulation in *Rupenyan et al.* [38], it was demonstrated that if the degree of alignment is 0.44, the minimum would occur at 60 eV, yet no experiment has ever been carried out on CO<sub>2</sub> molecules with such “poor” alignment with  $\langle \cos^2 \theta \rangle$  near 0.44.

In order to understand the origin of the discrepancy between the two experiments, we have carried out a “standard” QRS-type calculation. Through simulations, we have identified the plausible reason for the discrepancy in the position of minimum of the two experiments. More importantly, we have further found that the position and the depth of harmonic minimum are extremely sensitive to the alignment degree of CO<sub>2</sub>, especially when molecules are only slightly aligned for  $\langle \cos^2 \theta \rangle$  as close to 0.40 if the molecules are parallelly aligned. Recall that there is no deep minimum in the interested spectral region in the harmonic spectra if the molecules are isotropically distributed, i.e.,  $\langle \cos^2 \theta \rangle = 0.33$ . We have traced the origin of such strong alignment dependence to the strong angular dependence in the PR transition dipole moment of CO<sub>2</sub>, in particular, the position of a minimum that is very deep and narrow, and varies rapidly with the orientation of the molecular axis.

Recall that discrete harmonics can be synthesized to form an attosecond pulse train (APT) while synthesizing continuous harmonics can form an isolated attosecond pulse (IAP). Once attosecond pulses are generated in the gas medium, it is rather difficult to reshape the pulse without significant loss of its intensity. In view of the strong dependence of harmonic spectra on the alignment degree of CO<sub>2</sub>, we propose to use this property as a practical method to generate shaped attosecond pulses. As reported below, in Sec. II, we first show how we can interpret the discrepancy of the position of minimum in two experiments, and why such difference is special to CO<sub>2</sub>. We then show how the deep minimum in the harmonic

spectra can be manipulated by fine tuning the degree of alignment. In Sec. III, we examine features of attosecond pulses in the time domain to demonstrate how they would vary with the degree of alignment. To confirm that such predictions indeed happen, we show how to determine the phases of such harmonics, focusing on the IAPs, with the new phase retrieval method developed recently. The retrieval of spectral phases for shaped APTs is then addressed. We also discuss the possibility of generating shaped attosecond pulses experimentally. The last section provides a short summary of the present work.

## II. UNUSUAL FEATURES OF HARMONIC GENERATION FROM MODERATELY ALIGNED CO<sub>2</sub> MOLECULES

### A. Origin of the difference in the harmonic spectra between two seemingly identical experiments

In earlier experiments, HHG of CO<sub>2</sub> molecules were typically carried out using laser wavelength in range of 800 nm to about 1.3  $\mu\text{m}$ . To obtain a broad range of harmonics, higher laser intensities were often used. In such experiments, the position of the harmonic minimum tends to change with laser intensity resulting from interference of harmonics from multiple orbitals [30, 33]. In this work we focus on mid-infrared driving lasers that have wavelength longer than 1.4  $\mu\text{m}$ . Because of the wavelength  $\lambda^2$ -scaling of the cutoff energy of harmonics, a broad spectral range can be obtained without very high laser intensity such that the primary contribution to HHG comes from the HOMO, with little from inner molecular orbitals. According to the QRS model, in this limit one expects the position of the harmonic minimum to be independent of either the laser intensity or wavelength. Indeed, in *Vozzi et al.* [35], harmonic spectra of CO<sub>2</sub> using wavelengths of 1450, 1600, and 1700 nm were reported with several intensities around  $1.0 \times 10^{14}$  W/cm<sup>2</sup>. They found a clear deep minimum at about 60 eV and its position is independent of the laser intensity or wavelength. In a subsequent paper, *Rupenyan et al.* [38] reported the harmonic spectra from CO<sub>2</sub> molecules using wavelengths ranging from 1.16 - 1.46  $\mu\text{m}$ , with the alignment factor of  $\langle \cos^2 \theta \rangle = 0.54 - 0.64$ . Their 1.46  $\mu\text{m}$  laser parameters match with those used in *Vozzi et al.* [35], but the position of the minimum was found to be around 47 eV. In both experiments, the molecules are aligned by a weaker pump laser and the harmonic spectra are generated by a more intense and shorter probe laser. The two lasers are polarized along the same direction and the molecular alignment degrees were both reported to be  $\langle \cos^2 \theta \rangle = 0.60$ . Why do the positions of the minimum in the two experiments differ so much even with the same laser parameters and molecular alignment? In *Rupenyan et al.* [38] a theoretical calculation similar to the QRS theory was carried out in the single-molecule response level, and the position of the minimum at  $\langle \cos^2 \theta \rangle$

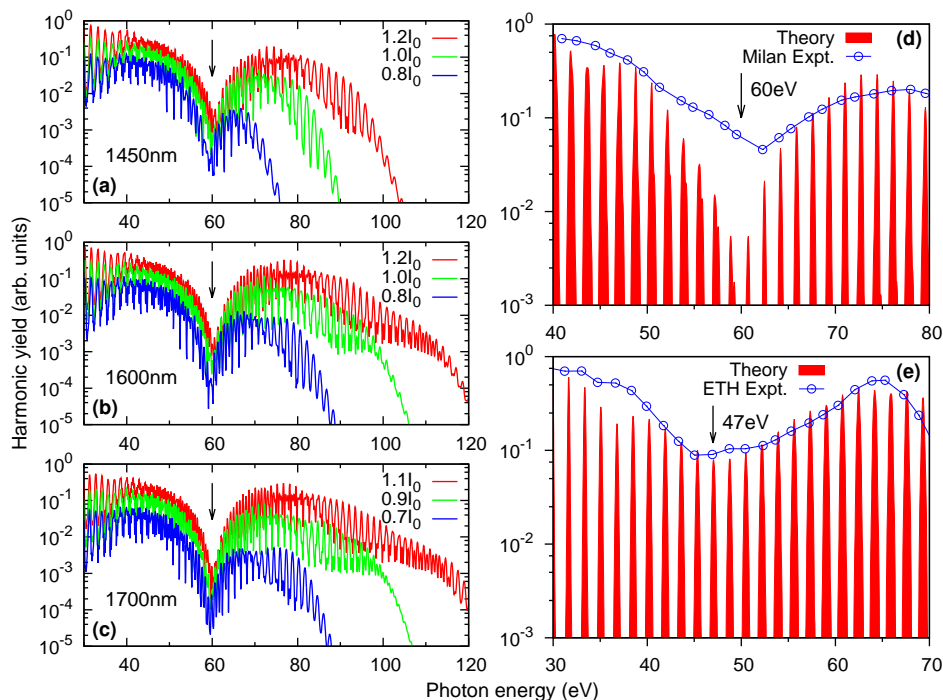


FIG. 1: (a)-(c) Simulated HHG spectra of aligned CO<sub>2</sub> molecules at different laser intensities and wavelengths (to be compared to Fig. 3 in Ref. [35]). In each figure, the laser intensity for individual spectrum is gradually decreased from top to bottom. Laser intensities at the center of gas jet are indicated with  $I_0 = 10^{14}$  W/cm<sup>2</sup>. Degree of alignment by a pump laser is  $\langle \cos^2 \theta \rangle = 0.40$ . (d)-(e) Comparison of theoretical HHG spectra and experimental ones of *Vozzi et al.* [35] and *Rupenyan et al.* [37] by using 1.45- and 1.46- $\mu$ m lasers, respectively.  $\langle \cos^2 \theta \rangle = 0.40$  in (d) and 0.55 in (e) in the simulations. The simulated results in (d) and (e) are smoothed by using the gaussian function (with a full-width-at-half-maximum of 0.3 times the fundamental frequency) centered in the odd harmonics. Both the HOMO and two inner orbitals are included in the simulations. Arrows indicate the positions of the deep minima. See text for additional laser parameters.

= 0.60 was found at 47 eV, in agreement with their experiment. In the meanwhile, their simulation indicates that a minimum at 60 eV occurs if  $\langle \cos^2 \theta \rangle = 0.44$ .

To investigate the discrepancy between the two experiments, we perform our “standard” QRS simulations. Different from the calculation of *Rupenyan et al.* [38], we use more accurate PR transition dipole matrix elements where the many-electron correlation has been better accounted for [46–48]. We also incorporate the propagation effect of harmonics generated in the gas medium [51]. In the simulations, we choose a pulse with duration of four optical cycles. Laser beam waist is assumed to be  $w_0 = 35$   $\mu$ m, and the gas length is 0.5 mm. The gas, uniformly distributed in the interaction region, is placed at 3 mm after the laser focus. These parameters are close to those used experimentally in *Vozzi et al.* [35]. Our simulation results are displayed in the left column of Fig. 1. They are to be compared to Fig. 3 of *Vozzi et al.* [35]. It is shown that the position of minimum does not change with either the laser intensity or wavelength. In addition, as illustrated in Fig. 2, the position of minimum does not change with laser focusing condition, nor affected by the contribution from HOMO-1 or HOMO-2 orbital, except that the depth of minimum is reduced. Most importantly, however, our simulation suggests that

minimum occurs at 60 eV with the alignment degree of 0.40, close to 0.44 as used in *Rupenyan et al.* [38].

To thoroughly compare our simulated spectra with those from *Vozzi et al.* [35], in Fig. 1(d), we display the envelope from each, including propagation effect, by using alignment factor of  $\langle \cos^2 \theta \rangle = 0.40$ . The position of minimum agrees quite well, but the depth of minimum from the simulation is significantly deeper by one order. Such discrepancy was not expected. Interestingly, when we compare our simulation with the data of *Rupenyan et al.* [38], not only the position of the minimum, but also the envelope, are in “perfect” agreement with data, when we use  $\langle \cos^2 \theta \rangle = 0.55$ , see Fig. 1(e).

To figure out the possible factor(s) contributing to the discrepancy between ours and the one from *Vozzi et al.* [35], we next look into the conditions of aligning lasers in the two experiments. Although the same  $\langle \cos^2 \theta \rangle = 0.6$  is utilized, three other parameters are different in *Vozzi et al.* [35] and in *Rupenyan et al.* [38], including the peak intensity ( $4.0$  vs  $0.4 \times 10^{13}$  W/cm<sup>2</sup>), the temperature of gas jet (75 vs 40 K), and the pulse duration (100 vs 120 fs). In particular, to reach the cited high intensity, the aligning laser in *Vozzi et al.* [35] is focused. Aiming to test the effect of a focused aligning laser on harmonic generation, we carry out simulations that account for the

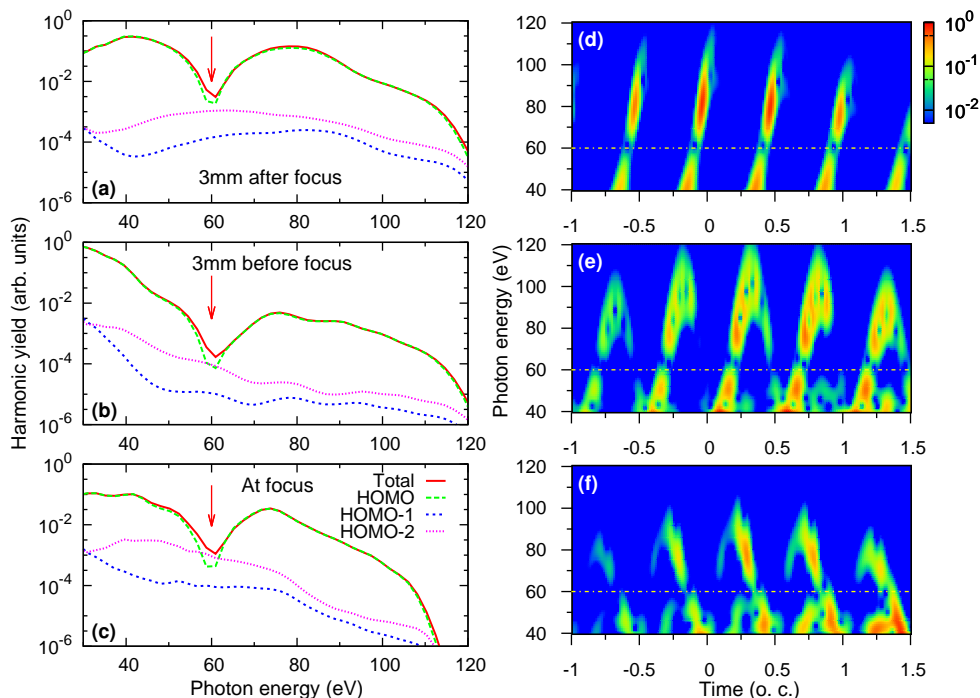


FIG. 2: (a)-(c) Simulated HHG spectra of aligned CO<sub>2</sub> molecules under different macroscopic conditions. In each figure, the total (HOMO, HOMO-1, and HOMO-2 together) spectra and individual HOMO, HOMO-1, and HOMO-2 spectra are plotted. To avoid the overlap of real HHG spectra, they are smoothed by using the method of Bezier curves. Laser wavelength is 1600 nm, peak laser intensity at the center of the gas jet is fixed at  $1.2 \times 10^{14}$  W/cm<sup>2</sup>. The positions of the gas jet with respect to laser focus are changed as indicated. Other parameters are the same as those in Fig. 1(b). (d)-(f) Time-frequency analysis of macroscopic harmonic emissions at off-axis position ( $r = w_0/3$ ) of exit plane at three different macroscopic conditions.  $w_0$  is the beam waist of the generating laser. (o.c. means the optical cycle of the 1600-nm laser.)

laser intensity distribution at the gas jet position using three different beam waists to represent different degrees of focusing, where the peak intensity at the focus is  $4 \times 10^{13}$  W/cm<sup>2</sup>. The simulation results are shown in Fig. 3. For the tight-focusing condition (beam waist  $w_0 = 20$   $\mu$ m) the harmonic minimum indeed occurs at about 60 eV. As the beam waist is increased, the position of minimum is shifted to about 50 eV ( $w_0 = 35$   $\mu$ m), close to the 47 eV as observed in Rupenyan *et al.* [38]. Thus, for the first time the origin of the discrepancy in the position of harmonic minimum between the two experiments is provided. In the meanwhile, the discrepancy of shallower minimum in the experimental data as compared to the much deeper minimum in the simulation in Fig. 1(d) can be understood. If the harmonic spectra were generated with molecules that are uniformly aligned with  $\langle \cos^2 \theta \rangle = 0.40$ , then the harmonic minimum is expected to be as deep as the one seen in the simulation. But no such measurements have been reported so far. In addition, the simulation also predicts that the position of minimum shifts rapidly with a small change in the degree of alignment. These strong alignment dependence owes to the properties of the photoionization transition dipole moments in CO<sub>2</sub>, as we further discuss below. This property offers the opportunity to control harmonic spectra using moderately aligned CO<sub>2</sub> molecules.

## B. Efficient control of harmonic spectra by tuning the alignment of CO<sub>2</sub> molecules

The simulation of experimental harmonic spectra from partially aligned molecules involves the following steps. First, one calculates

$$d^{\parallel, \text{avg}}(\omega, \alpha) = \int_0^\pi N(\theta)^{1/2} d^{\parallel}(\omega, \theta) \rho(\theta, \alpha) \sin \theta d\theta. \quad (1)$$

Here  $d^{\parallel, \text{avg}}(\omega, \alpha)$  is the averaged PR transition dipole,  $N(\theta)$  is the ionization probability [49, 50],  $\rho(\theta, \alpha)$  is the alignment distribution (in the probe-laser frame) for the pump-probe angle  $\alpha$ , and  $d^{\parallel}(\omega, \theta)$  is the parallel (to the probe laser polarization) component of the PR transition dipole. A similar expression can be written for the perpendicular polarization direction. Here we consider  $\alpha = 0^\circ$  only so there is no perpendicular polarization component. Notice that the average transition dipole for each molecule is calculated coherently. With  $d^{\parallel, \text{avg}}(\omega, \alpha)$  calculated, in the second step the harmonics generated in the gas medium are obtained by solving the Maxwell's wave equations [51] to account for the effect of phase matching. Since  $d(\omega)$  does not depend on the laser [22], the observed harmonic spectrum can still be written in a product form, where the wave packet  $W(\omega)$  in the QRS theory is replaced by a volume integrated

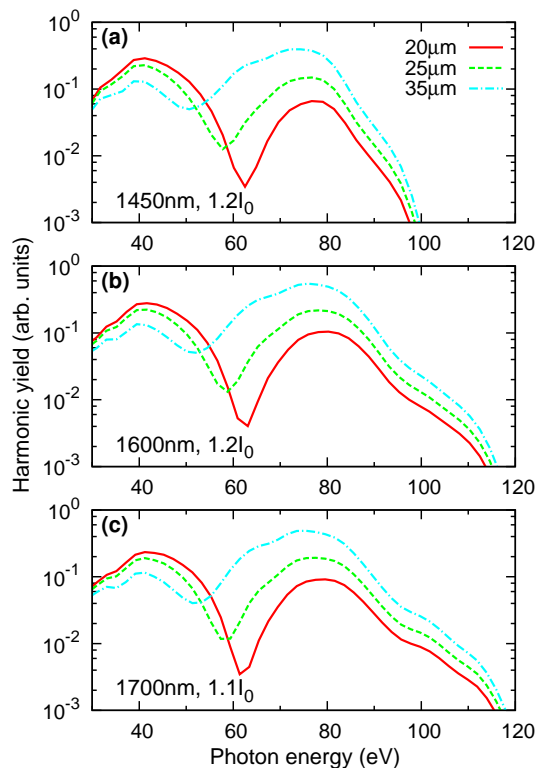


FIG. 3: Simulated HHG spectra of aligned  $\text{CO}_2$  molecules under different focusing conditions of the pump laser. The spectra were smoothed by using Bezier curves. The wavelength of the pump laser is 800 nm, its intensity at the focus is fixed at  $0.4 \times 10^{14} \text{ W/cm}^2$ , and its beam waist is varied as indicated in the figures. The 0.5-mm long gas jet is located 3 mm after the laser focus. The wavelength and intensity (at the center of gas jet) of probe laser are labeled in the figures. Other macroscopic conditions for the probe laser are the same as those in Fig. 1 (b).

wave packet  $W'(\omega)$  which varies smoothly with photon energy. The macroscopic harmonic yields generated from a single molecular orbital can then be expressed as [51]

$$S_h^{\parallel}(\omega, \alpha) \propto \omega^4 |W'(\omega)|^2 |d^{\parallel, \text{avg}}(\omega, \alpha)|^2, \quad (2)$$

where  $W'(\omega)$  is called a “macroscopic wave packet” (MWP). Thus, according to the QRS theory, the position of the minimum in the experimental harmonic spectra is determined by the angular distribution weighted transition dipole moment in Eq. (1).

Fig. 4(a) shows the modulus square of the PR transition dipole for a fixed-in-space  $\text{CO}_2$  molecule at a few angles from  $40^\circ$  to  $60^\circ$ . Note that the position of minimum and the amplitude change rapidly with the fixed-in-space angle. At the same time, the phase of the dipole undergoes a change of  $\pi$  within a small energy range, the narrower the minimum in Fig. 4(a), the smaller the energy range. Fig. 4(d) shows how the averaged transition dipole and phase look like after the convolution with angular distribution for the case of  $\langle \cos^2 \theta \rangle = 0.40$ . In a narrow energy region near the minimum, both the ampli-

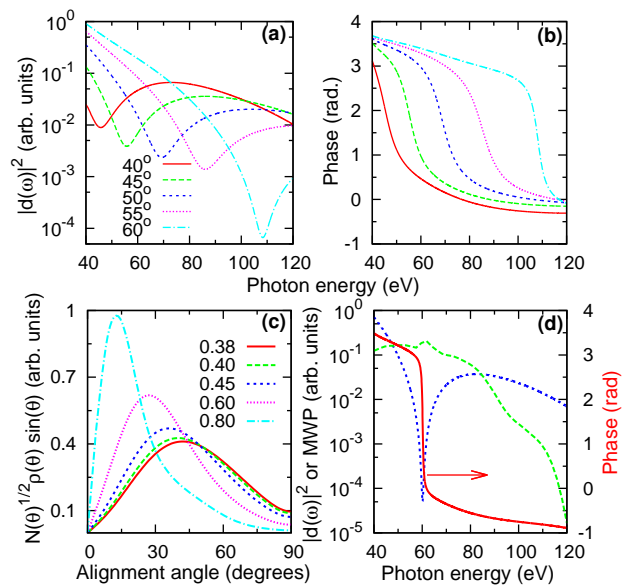


FIG. 4: Photoionization transition dipole moment (the modulus square) (a) and phase (b) of fixed-in-space  $\text{CO}_2$  molecules at selected alignment angles. Only the parallel component to the polarization direction of laser is shown. (c) Weighted angular distributions at different degrees of alignment by including the ionization rate  $N(\theta)$  and alignment distribution  $\rho(\theta)$ . (d) Averaged photoionization transition dipole (the modulus square, blue short dashed line), phase of the dipole (red solid line), and the modulus square of the macroscopic wave packet (MWP) (green long dashed line) of the HOMO extracted from HHG spectra (1600 nm,  $1.2 I_0$ ) shown in Fig. 1(b).

tude and phase of the averaged transition dipole change dramatically in a narrow photon energy region. In contrast, the wave packet varies slowly with photon energy in the same energy region. Fig. 4(c) shows the angular distributions weighted by the alignment-dependent ionization probability. While they do not change significantly for  $\langle \cos^2 \theta \rangle = 0.38$  to  $0.45$ , Fig. 5(a) shows that the modulus square of the averaged transition dipole changes significantly, where the position of minimum moves from 63 to 55 eV, and in each case it is accompanied by a large change of phase, as shown in Fig. 5(b).

We emphasize that the averaged transition dipole shown in Fig. 4(d) is for molecules that are partially aligned along zero degree with respect to the probe laser. For  $\langle \cos^2 \theta \rangle = 0.4$ , for example, the averaged transition dipole gets significant contributions from a broad angular range, see Fig. 4(c). In fact, for fixed-in-space molecules, the transition dipole can have a minimum only when the orientation angle of the molecule is within a range of  $30^\circ$  to  $60^\circ$ . Thus the minima in Fig. 5(a) for different degrees of alignment are caused predominately by the coherent superposition of transition dipole in that angular range. If the molecules are well aligned, then there would be no minimum in the averaged transition dipole. It can be seen already for  $\langle \cos^2 \theta \rangle = 0.50$ , as seen in Fig. 5(a). This figure also shows why the position and depth of the

minima in the averaged transition dipole are so sensitive to the degree of alignment. We mention that Fig. 5(a) would mimic the harmonic spectra since the macroscopic wave packet is a smooth function of photon energy.

### III. FEATURES OF ATTOSECOND PULSES SYNTHESIZED FROM A HARMONIC SPECTRUM THAT CONTAINS A DEEP MINIMUM

#### A. Efficient shaping of attosecond pulses

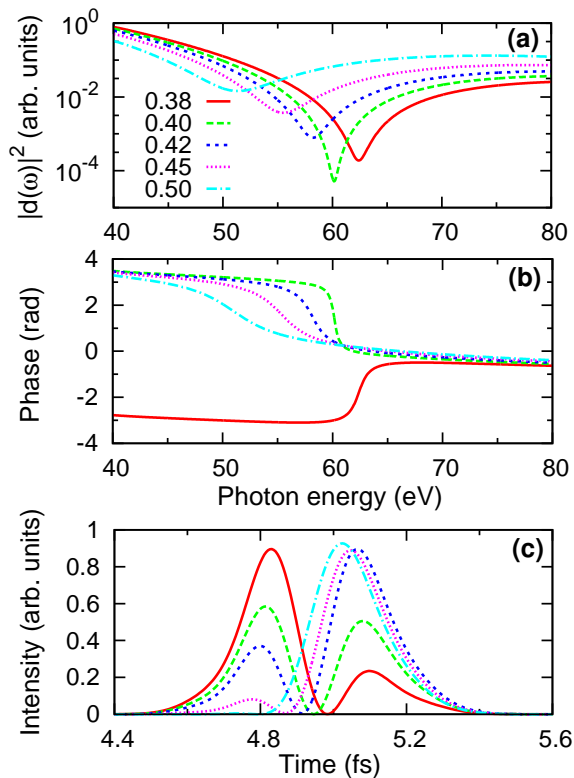


FIG. 5: (a) Averaged photoionization transition dipoles (the modulus square); (b) their phases, for the HOMO and parallel component only. Alignment degrees are indicated. (c) Attosecond pulses synthesized by off-axis ( $r = w_0/3$ ) harmonics from 55 to 65 eV. Gaussian envelope is applied to harmonics lower (or higher) than boundary ones. The results obtained from higher alignment degrees in (c) have been multiplied by some factors for easy comparison. The high harmonics are obtained by including both HOMO and two inner orbitals, and other macroscopic conditions are the same as those in Fig. 1(b) for 1600 nm and  $1.2 I_0$ .

The previous section focuses on the harmonic spectra near the energy range where the minimum in the spectrum is very pronounced. Considering harmonics calculated from a 1600-nm laser with the duration of four optical cycles, we synthesize the ones covering from 55 - 65 eV which include the harmonic minimum. Fig. 5(c) shows the time profile of resulting attosecond pulses over

one-half optical cycle. (The time profiles at other half cycles are similar, see Fig. 6.) Here, the time-domain attosecond pulses show two peaks within each half-cycle, in contrast to attosecond pulses that have only one single peak if the harmonics do not contain a minimum. Very clearly, the relative contrast between the two peaks depends sensitively on the degree of alignment, consistent with the similar sensitive dependence of the harmonic spectra. This figure illustrates that one can change the temporal profile of attosecond pulses readily just by simply tuning the degree of alignment slightly. Note that the harmonic spectra were taken from Fig. 2(a) using focusing conditions that long-trajectory electrons have been removed through good phase matching.

The results presented in Fig. 5(c) are based on simulations with known alignment of molecules. One may argue that in experiments the precise alignment is not known such that the predicted shaping of attosecond pulses cannot be realized. This is not true. The degree of alignment can be readily adjusted by changing the input power of pump laser. It is straightforward for experimentalists to locate the existence of harmonic minimum without knowing the precise probe pulse intensity (since the position of minimum does not depend on the intensity of probing laser). To find the pump laser that would provide the deepest minimum one can just directly look at the harmonic spectra as it is tuned. This is most easily carried out experimentally either by adding an iris in front of the pump laser to fine tune its input power, or by slightly adjusting the relative fraction of the pump and probe lasers' input power (or by somewhat adjusting the time delay between the two lasers). Fig. 7 presents some simulation results. For gas temperature of 30 to 50 K, a pump laser intensity below  $1.2 \times 10^{12}$  W/cm<sup>2</sup> can already cover the alignment in the desired range.

#### B. Characterization of shaped isolated attosecond pulses

To demonstrate shaped attosecond pulses in the time domain, it is best performed with isolated attosecond pulses (IAPs). We illustrate this with theoretically constructed IAPs. As given in Eq. (2), an IAP can be theoretically constructed in the energy domain, for example, through multiplying a continuous Gaussian (or any) envelope by  $d(\omega)$ , which has the known amplitude and phase [as given in Figs. 5(a) and (b)].

The method of characterizing shaped attosecond pulses is not different from the one used to characterize IAPs generated in atoms. Both the amplitude and phase of the harmonics have to be known. The amplitude can be deduced from the photoelectron spectra for simple atoms ionized by the attosecond pulse alone, while the spectral phase can be determined by measuring the so-called streaking spectra generated by atoms in the combined field of the attosecond pulse and a moderately intense infrared laser. By analyzing the photoelectron

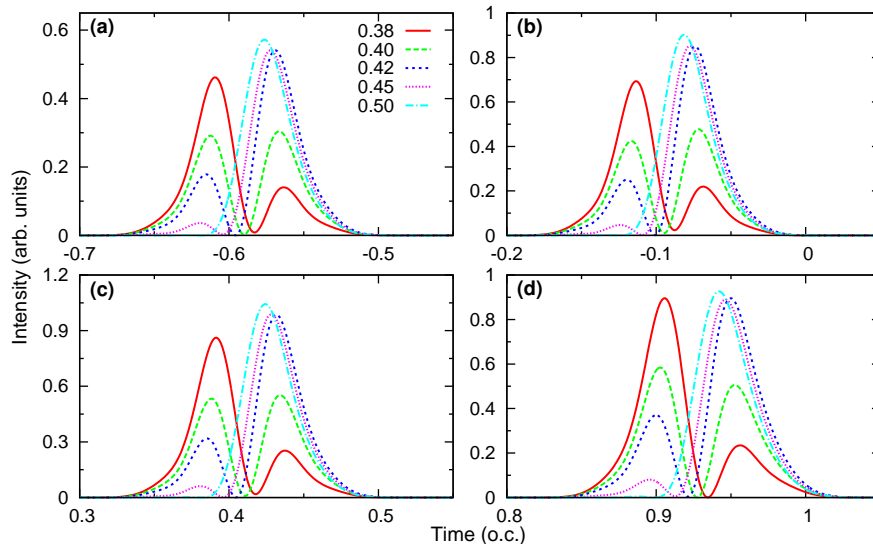


FIG. 6: Attosecond pulses shown in different half optical cycles by synthesizing off-axis ( $r = w_0/3$ ) harmonics at the exit plane from 55 to 65 eV with only molecular alignment distribution being adjusted. Gaussian envelope functions are applied to harmonics lower than 55 eV and higher than 65 eV. The results for  $\langle \cos^2 \theta \rangle = 0.45$  and  $0.50$  have been multiplied by  $1/2$  and  $1/5$  for easy comparison. (o.c. stands for optical cycle of the 1600-nm laser.) Other macroscopic conditions are the same as those in Fig. 1(b).

spectra versus the time delay between the two pulses, the spectral phase of attosecond pulses has been reliably retrieved using the FROG-CRAB method. However, a better method called PROBP [52] has been demonstrated since the latter removes the so-called central momentum approximation. (The PROBP-AC method [53] developed most recently is for broadband pulses so it is not needed here.) In the following, we demonstrate how to retrieve the three shaped attosecond pulses that are generated from  $\text{CO}_2$  molecules with slightly different degrees of alignment.

The electric field of an IAP (in frequency domain) is described by  $U(\omega)\exp[i\Phi(\omega)]$ , where the amplitude is  $U(\omega) = |d(\omega)| \times E_0 e^{-(\omega-\omega_0)^2/(\Delta\omega)^2}$ , and the phase is directly taken from  $d(\omega)$  as shown in Fig. 5(b). The central frequency  $\omega_0$  is set to be the dip position of the modulus of the transition dipole moment  $d(\omega)$ . The amplitudes of  $U(\omega)$  are plotted in Figs. 8 (a)-(c) for the three cases of  $\langle \cos^2 \theta \rangle = 0.4, 0.42$ , and  $0.5$ , and the phases of  $\Phi(\omega)$  and the corresponding temporal intensity envelopes of IAPs are shown in Fig. 9 (blue solid lines). We use such IAP fields combined with a moderate 800-nm laser to interact with Ar atom, and the resulted photoelectron spectrograms are shown in Figs. 8(d)-(f), simulated by using the strong-field approximation (SFA). A minimum band is formed near the central frequency subtracted by the ionization potential of Argon, where electrons could hardly be emitted. The minimum positions for  $\langle \cos^2 \theta \rangle = 0.4, 0.42$ , and  $0.5$  are around 44 eV, 42 eV, and 35 eV, respectively. Similar spectrograms have also been examined in Ref. [54], where the minimum band originates from the phase jump in the transition dipole moment of the target atom.

To retrieve the spectral phase of the IAP pulse from the spectrogram, we apply the PROBP method [52]. The spectral phase is expanded using B-spline basis functions. In addition to the size of the basis set ( $n$ ) and the numbers of knots ( $n+k$  in the case without multiplicity, where  $k$  is the order of B-splines), which have been discussed in Ref. [52], the multiplicity and the distribution of knots are explored here. Including multiplicities to the end knots ensure that a non-zero value of the target function at boundaries is taken into account. The multiplicity increases the size of the knot points from  $(n+k)$  to  $(n+k+m_1+m_2)$ , where  $m_1$  ( $m_2$ ) is the multiplicity of the first (last) knot. In the following, we focus on  $m_1 = m_2 = m$ . Besides multiplicity, distribution of the knot points is important in order to effectively describe a drastic change in a target function without using too many basis functions. A non-uniform placement of the knots is adopted in replacement of the uniform distribution used in Ref. [52]. The non-uniformity is controlled by a parameter  $\alpha$ , which generates an exponentially increasing grid spacing as we move away from the central frequency of  $\omega_0$ . With these two features included, the pre-optimization process of the basis functions becomes a scan through the parameter set of  $\{n, k, m, \alpha\}$ . The most favorable basis set, which gives the optimum fitness within around 100 generations, is then used for the second-stage optimization to find the expansion coefficients of that basis set. For our retrieval, the number/order of B-spline basis functions are  $n = 9$  and  $k = 4$ , and the multiplicity of the end knots is the same as the B-spline order, i.e.  $m = 4$ .

Figs. 9(a), (c), and (e) show our retrieved results of the spectral phases for  $\langle \cos^2 \theta \rangle = 0.4, 0.42$ , and  $0.5$  (orange



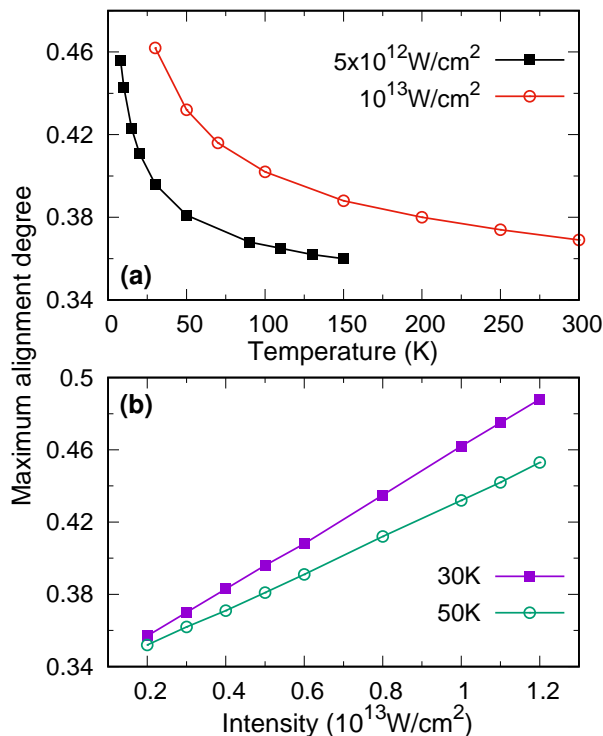


FIG. 7: Calculated maximum value of the alignment degree ( $\cos^2 \theta$ ) at the first half-revival as a function of gas temperature (a) or laser intensity (b). The aligning laser has a wavelength of 800 nm and duration of 100 fs. The laser intensities in (a) and gas temperatures in (b) are fixed, respectively.

dashed lines), respectively, in comparison with the input spectral phases (blue solid lines). The phase jumps in all three cases are reconstructed faithfully with the PROBP method except in the energy regions where the spectral amplitude is small. The input (blue solid lines) and the reconstructed temporal intensity profiles (orange dashed lines) calculated by using the input and retrieved spectral amplitudes and phases are shown in Figs. 9 (b), (d), and (f). Good agreement is reached.

The phase characterization method demonstrated here for theoretical streaking spectra can be applied to analyze experimental data to retrieve shaped isolated attosecond pulses. Pulses similar to Figs. 9(b), (d), and (f) can be generated simply just by fine tuning the alignment degree of the pump laser on  $\text{CO}_2$  molecules. By changing the wavelength or the intensity of probe laser would not change the shaped attosecond pulses. The strong variation of attosecond pulses generated here by slightly tuning the degree of molecular alignment can be viewed as a dramatic demonstration of coherent control since the effect relies on the coherence of harmonics generated from all molecules in the gas medium. The effect is dramatic because the phase of transition dipole varies rapidly through  $\pi$  in  $\text{CO}_2$  near the minimum of transition dipole matrix element. Such large phase change cannot be achieved using external phase modulators.

### C. Retrieval of the phase of shaped attosecond pulse train using the RABITT method

Here we show how to retrieve the phase of split attosecond pulse trains from experimental data to reconstruct their temporal profiles as displayed in Fig. 6. The so-called RABITT (reconstruction of attosecond beating by interference of two-photon transitions) [55] method is often used for retrieving the spectral phase of discrete harmonics. Experimentally, photoelectron spectra generated by the APT in the presence of a moderate IR pulse at different delay times are recorded. The electron spectra versus time delay would appear like those shown in Fig. 10. Besides the odd harmonics, even harmonics, called sidebands, would appear. The sideband signals show modulation which can be expressed as

$$S_{2q} = A_{2q} + B_{2q} \cos[2\omega_{IR}t_d - (\varphi_{2q+1} - \varphi_{2q-1}) - \Delta_{2q}^{atomic}]. \quad (3)$$

One can see that  $S_{2q}$  oscillates with frequency  $2\omega_{IR}$  as a function of APT-IR time delay  $t_d$ . The atomic phase  $\Delta_{2q}^{atomic}$  is usually small compared to the phase of the harmonics, and is neglected here. We thus can determine the phase difference  $\varphi_{2q+1} - \varphi_{2q-1}$  between two adjacent odd harmonics by fitting the oscillation of sideband signal.

In the absence of experimental streaking spectra for shaped APT presented in this article, we generate the streaking spectra using the strong-field approximation (SFA). The infrared field is given by  $E_{IR}(t) = E_{IR} e^{-t^2/\tau^2} \times \cos(\omega_{IR}t + \phi_{CEP})$ , where  $E_{IR}$  is the field strength,  $\omega_{IR} = 2\pi/\lambda$  is the angular frequency,  $\tau$  is the duration of the field, and  $\phi_{CEP}$  is the carrier envelope phase. For the shaped harmonic spectra, it is constructed by using the modulus of the averaged photoionization transition dipole in Fig. 5(a) multiplied by a discrete Gaussian envelope peaking at each odd harmonics of 800-nm laser, while keeping its phase, see the blue solid and orange dashed lines in 10(b), respectively. Applying the RABITT method, from Fig. 10(a), the retrieved phases at odd harmonics (orange solid circles) are shown in Fig. 10(b), which agree reasonably well with the input ones, and the fast  $\pi$  phase jump between harmonics 37 and 41 is demonstrated. Note that a better resolution of the retrieved phase jump can be obtained by using a longer-wavelength laser as the streaking field to reduce the IR photon energy between the orders [23].

## IV. CONCLUSIONS

In summary, we have identified a new alignment-induced enhancement of the minimum in high harmonic generation of  $\text{CO}_2$  molecules. While minima in the harmonic spectra are ubiquitous in molecules, the minima are in general not very deep and the phase change of harmonic across the minimum in general is less than  $\pi$ , for example, 2.7 radians at Cooper minimum in Ar [23] and

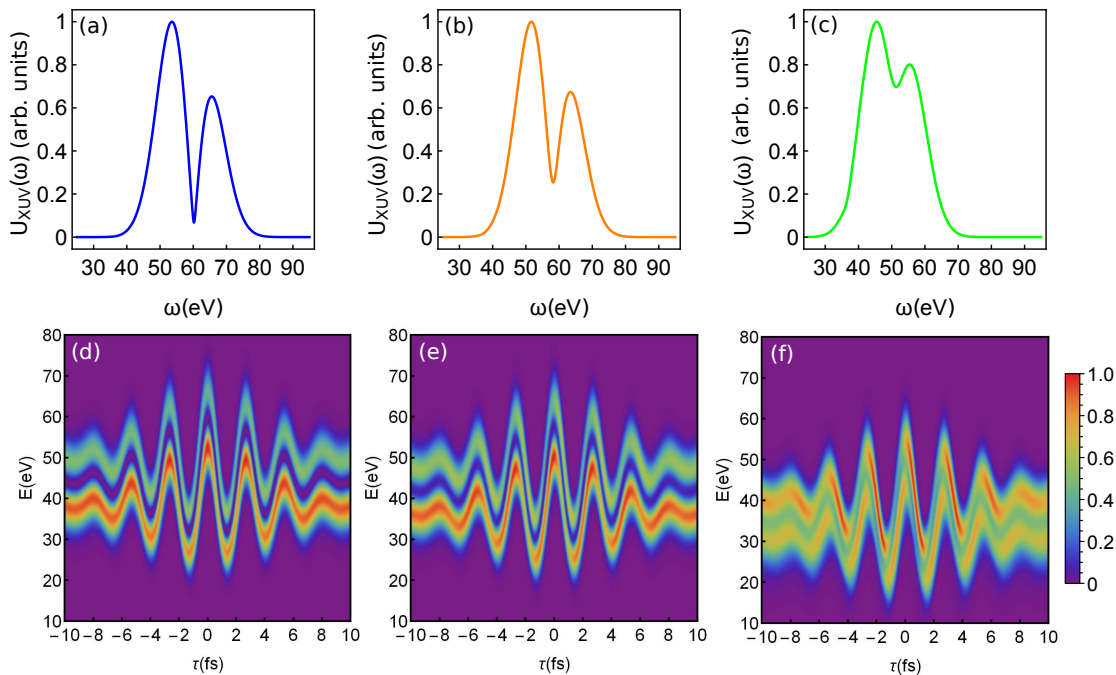


FIG. 8: Photoelectron spectrograms based on the SFA. Panels (a)-(c) show the actual IAP amplitudes used for generating the photoelectron spectrograms in (d), (e), and (f) for  $\langle \cos^2 \theta \rangle = 0.4, 0.42, \text{ and } 0.5$ , respectively. The IAP bandwidth  $\Delta\omega = 10$  eV and  $I_{XUV} = 10^{12}$  W/cm<sup>2</sup>. For the streaking field, we use  $I_{IR} = 10^{13}$  W/cm<sup>2</sup>,  $\lambda = 800$  nm,  $\tau = 5.7$  fs, and  $\phi_{CEP} = \pi/2$ . The spectrograms are rescaled to the range of  $[0, 1]$ .

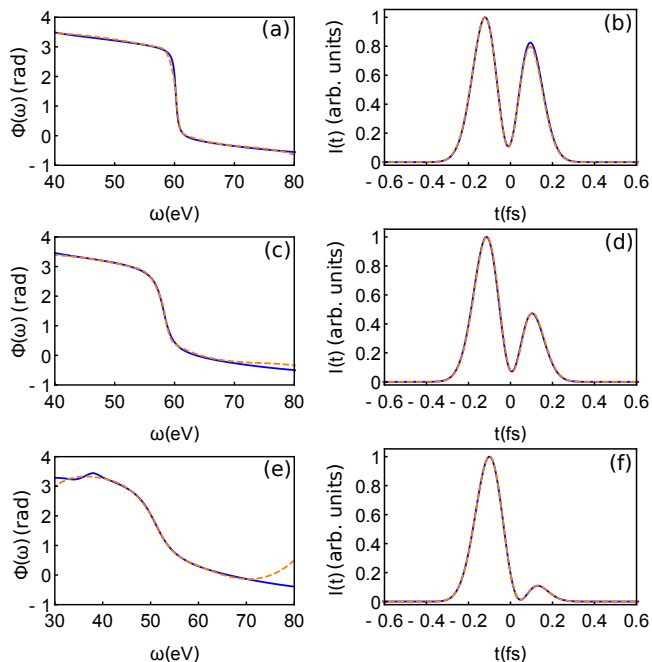


FIG. 9: Panel (a), (c), and (e) (the left column) show the input phases (blue solid lines) and the retrieved phase (orange dashed lines) for  $\langle \cos^2 \theta \rangle = 0.4, 0.42, \text{ and } 0.5$ , respectively. The retrieved results reproduce the input spectral phases well except in the energy regions where the spectral amplitude is small. Panels (b), (d), and (f) show the corresponding intensity profiles using the input phase and the retrieved phase.

at 48 eV in CO<sub>2</sub> [29], and 2.6 radians in CH<sub>3</sub>Cl [56]. It is also known that such large phase change in general will generate moderately shaped attosecond pulses as in the case of Ar [23]. What is different in this study is that the harmonic minima are much deeper and the phase undergoes a change over  $\pi$  in a relatively small energy region. Unlike the minimum in Ar, the minima discussed here are significantly enhanced because of the interference of harmonic minima from aligned molecules. Thus the position and depth of minima are very sensitive to the degree of alignment. This sensitivity offers a simple and practical method for shaping attosecond pulses by slightly changing the alignment degree of CO<sub>2</sub>. This method works at relatively small degree of alignment, thus they are easily realized in experiments.

While we have identified CO<sub>2</sub> as a working medium for efficient generation of shaped attosecond pulses, other molecules like N<sub>2</sub>O [38] which have deep harmonic minima probably work as an effective medium as well. In addition, we have considered parallel pump and probe polarizations in this article only, similar sensitive alignment dependence has been found for non-parallel configurations. In the latter cases, when minimum occurs for the parallel polarization harmonics, the perpendicular components in general will not be at the minimum. Thus, by exploiting the non-parallel pump-probe geometry the present method may be used to generate polarized shaped attosecond pulses [57] that can be easily tuned with the alignment degree of molecules. Such shaped attosecond pulses would provide new tools for probing ul-

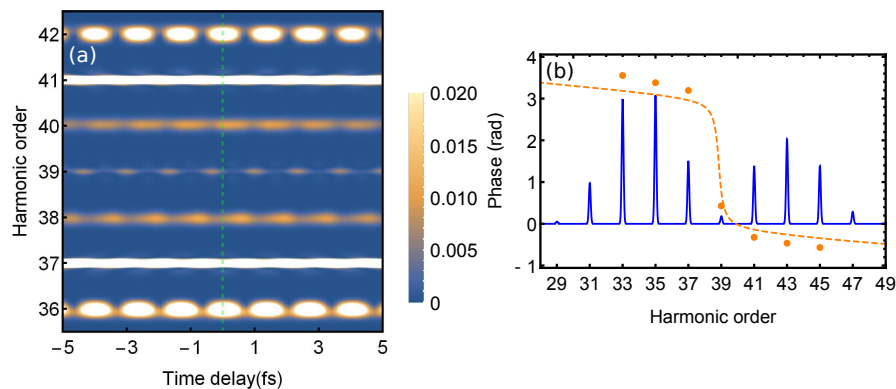


FIG. 10: (a) Photoelectron spectrum as a function of time delay. The green line connects two sideband maxima, which can guide the eye to see the change of the location of the other sideband maxima. (b) The retrieved phase at odd harmonics shown as orange solid circles by using RABITT method. Panel (b) also shows the input APT amplitudes (blue solid line) and phase (orange dashed line) for  $\langle \cos^2 \theta \rangle = 0.4$  that was used for generating the spectrum in (a). For the streaking field, we use  $I_{\text{IR}} = 10^{13}$  W/cm<sup>2</sup>,  $\lambda = 800$  nm,  $\tau = 5.7$  fs, and  $\phi_{\text{CEP}} = \pi/2$ . For easy comparison, we use the harmonic order (with respect to the 800-nm laser) to label photoelectron energy in (a), whose actual value equals the photon energy of high harmonic minus the ionization potential of target atom.

trafast electron dynamics and open up new opportunities in attosecond sciences.

## V. ACKNOWLEDGMENTS

We thank Dr. Caterina Vozzi and Dr. Giuseppe Sansone for fruitful discussions. C.J., X.Z. and S.-F.Z. were

supported by National Natural Science Foundation of China (NSFC) under Grants No. 11774175, 91950102, 11834004, 11904192, and 11664035. And S.-J.W., X.Z. and C.D.L. were supported by Chemical Sciences, Geosciences and Biosciences Division, Office of Basic Energy Sciences, Office of Science, U.S. Department of Energy under Grant No. DE-FG02-86ER13491.

- 
- [1] F. Krausz and M. Ivanov, “Attosecond physics,” *Rev. Mod. Phys.* **81**, 163-234 (2009).
- [2] L.-Y. Peng, W.-C. Jiang, J.-W. Geng, W.-H. Xiong, and Q. Gong, “Tracing and controlling electronic dynamics in atoms and molecules by attosecond pulses,” *Phys. Rep.* **575**, 1-72 (2015).
- [3] F. Calegari, G. Sansone, S. Stagira, C. Vozzi, and M. Nisoli, “Advances in attosecond science,” *J. Phys. B* **49**, 062001 (2016).
- [4] J. P. Marangos, “Development of high harmonic generation spectroscopy of organic molecules and biomolecules,” *J. Phys. B* **49**, 132001 (2016).
- [5] H. Yun, S. J. Yun, G. H. Lee, and C. H. Nam, “High-harmonic spectroscopy of aligned molecules,” *J. Phys. B* **50**, 022001 (2017).
- [6] P. M. Kraus and H. J. Wörner, “Perspectives of Attosecond Spectroscopy for the Understanding of Fundamental Electron Correlations,” *Angew. Chem. Int. Ed.* **57**, 2-22 (2018).
- [7] P. M. Paul, E. S. Toma, P. Breger, G. Mullot, F. Augé, Ph. Balcou, H. G. Muller, and P. Agostini, “Observation of a Train of Attosecond Pulses from High Harmonic Generation,” *Science* **292**, 1689-1692 (2001).
- [8] M. Hentschel, R. Kienberger, C. Spielmann, G. A. Reider, N. Milosevic, T. Brabec, P. Corkum, U. Heinzmann, M. Drescher, and F. Krausz, “Attosecond metrology,” *Nature* **414**, 509-513 (2001).
- [9] A. Kaldun, A. Blättermann, V. Stooß, S. Donsa, H. Wei, R. Pazourek, S. Nagele, C. Ott, C. D. Lin, J. Burgdörfer, and T. Pfeifer, “Observing the ultrafast buildup of a Fano resonance in the time domain,” *Science* **354**, 738-741 (2016).
- [10] Y. Pertot, C. Schmidt, M. Matthews, A. Chauvet, M. Huppert, V. Svoboda, A. von Conta, A. Tehlar, D. Baykusheva, J.-P. Wolf, and H. J. Wörner, “Time-resolved x-ray absorption spectroscopy with a water window high-harmonic source,” *Science* **355**, 264-267 (2017).
- [11] J. L. Krause, K. J. Schafer, and K. C. Kulander, “High-order harmonic generation from atoms and ions in the high intensity regime,” *Phys. Rev. Lett.* **68**, 3535-3538 (1992).
- [12] P. B. Corkum, “Plasma perspective on strong field multiphoton ionization,” *Phys. Rev. Lett.* **71**, 1994-1997 (1993).
- [13] A. T. Le, R. R. Lucchese, S. Tonzani, T. Morishita, and C. D. Lin, “Quantitative rescattering theory for high-order harmonic generation from molecules,” *Phys. Rev. A* **80**, 013401 (2009).
- [14] C. D. Lin, A. T. Le, C. Jin, and H. Wei, “Elements of the quantitative rescattering theory,” *J. Phys. B* **51**, 104001 (2018).
- [15] C. D. Lin, A. T. Le, C. Jin, and H. Wei, “Attosecond and Strong-Field Physics: Principles and Applications,” (Cambridge University Press, 2018), pp. 209-213.

- [16] H. J. Wörner, H. Niikura, J. B. Bertrand, P. B. Corkum, and D. M. Villeneuve, "Observation of Electronic Structure Minima in High-Harmonic Generation," *Phys. Rev. Lett.* **102**, 103901 (2009).
- [17] S. Minemoto, T. Umegaki, Y. Oguchi, T. Morishita, A. T. Le, S. Watanabe, and H. Sakai, "Retrieving photorecombination cross sections of atoms from high-order harmonic spectra," *Phys. Rev. A* **78**, 061402(R) (2008).
- [18] E. J. Takahashi, T. Kanai, Y. Nabekawa, and K. Midorikawa, "10 mJ class femtosecond optical parametric amplifier for generating soft x-ray harmonics," *Appl. Phys. Lett.* **93**, 041111 (2008).
- [19] P. Colosimo, G. Doumy, C. I. Baga, J. Wheeler, C. Hauri, F. Catoire, J. Tate, R. Chirla, A. M. March, G. G. Paulus, H. G. Muller, P. Agostini, and L. F. Dimauro, "Scaling strong-field interactions towards the classical limit," *Nat. Phys.* **4**, 386-389 (2008).
- [20] J. P. Farrell, L. S. Spector, B. K. McFarland, P. H. Bucksbaum, M. Gühr, M. B. Gaarde, and K. J. Schafer, "Influence of phase matching on the Cooper minimum in Ar high-order harmonic spectra," *Phys. Rev. A* **83**, 023420 (2011).
- [21] J. Higuier, H. Ruf, N. Thiré, R. Cireasa, E. Constant, E. Cormier, D. Descamps, E. Mével, S. Petit, B. Pons, Y. Mairesse, and B. Fabre, "High-order harmonic spectroscopy of the Cooper minimum in argon: Experimental and theoretical study," *Phys. Rev. A* **83**, 053401 (2011).
- [22] C. Jin, H. J. Wörner, V. Tosa, A. T. Le, J. B. Bertrand, R. R. Lucchese, P. B. Corkum, D. M. Villeneuve, and C. D. Lin, "Separation of target structure and medium propagation effects in high-harmonic generation," *J. Phys. B* **44**, 095601 (2011).
- [23] S. B. Schoun, R. Chirla, J. Wheeler, C. Roedig, P. Agostini, L. F. DiMauro, K. J. Schafer, and M. B. Gaarde, "Attosecond Pulse Shaping around a Cooper Minimum," *Phys. Rev. Lett.* **112**, 153001 (2014).
- [24] M. Lein, N. Hay, R. Velotta, J. P. Marangos, and P. L. Knight, "Role of the Intramolecular Phase in High-Harmonic Generation," *Phys. Rev. Lett.* **88**, 183903 (2002).
- [25] C. Vozzi, F. Calegari, E. Benedetti, J.-P. Caumes, G. Sansone, S. Stagira, M. Nisoli, R. Torres, E. Heesel, N. Kajumba, J. P. Marangos, C. Altucci, and R. Velotta, "Controlling Two-Center Interference in Molecular High Harmonic Generation," *Phys. Rev. Lett.* **95**, 153902 (2005).
- [26] T. Kanai, S. Minemoto, and H. Sakai, "Quantum interference during high-order harmonic generation from aligned molecules," *Nature* **435**, 470-474 (2005).
- [27] N. Wagner, X. Zhou, R. Lock, W. Li, A. Wüest, M. Murnane, and H. Kapteyn, "Extracting the phase of high-order harmonic emission from a molecule using transient alignment in mixed samples," *Phys. Rev. A* **76**, 061403(R) (2007).
- [28] T. Kanai, E. J. Takahashi, Y. Nabekawa, and K. Midorikawa, "Observing molecular structures by using high-order harmonic generation in mixed gases," *Phys. Rev. A* **77**, 041402(R) (2008).
- [29] W. Boutu, S. Haessler, H. Merdji, P. Breger, G. Waters, M. Stankiewicz, L. J. Frasinski, R. Taieb, J. Caillat, A. Maquet, P. Monchicourt, B. Carre, and P. Salieres, "Coherent control of attosecond emission from aligned molecules," *Nat. Phys.* **4**, 545-549 (2008).
- [30] O. Smirnova, Y. Mairesse, S. Patchkovskii, N. Dudovich, D. Villeneuve, P. Corkum, and M. Yu. Ivanov, "High harmonic interferometry of multi-electron dynamics in molecules," *Nature* **460**, 972-977 (2009).
- [31] P. Wei, P. Liu, J. Chen, Z. Zeng, X. Guo, X. Ge, R. Li, and Z. Xu, "Laser-field-related recombination interference in high-order harmonic generation from CO<sub>2</sub> molecules," *Phys. Rev. A* **79**, 053814 (2009).
- [32] H. J. Wörner, J. B. Bertrand, P. Hockett, P. B. Corkum, and D. M. Villeneuve, "Controlling the Interference of Multiple Molecular Orbitals in High-Harmonic Generation," *Phys. Rev. Lett.* **104**, 233904 (2010).
- [33] R. Torres, T. Siegel, L. Brugnera, I. Procino, J. G. Underwood, C. Altucci, R. Velotta, E. Springate, C. Froud, I. C. E. Turcu, S. Patchkovskii, M. Yu. Ivanov, O. Smirnova, and J. P. Marangos, "Revealing molecular structure and dynamics through high-order harmonic generation driven by mid-IR fields," *Phys. Rev. A* **81**, 051802(R) (2010).
- [34] C. Jin, A. T. Le, and C. D. Lin, "Analysis of effects of macroscopic propagation and multiple molecular orbitals on the minimum in high-order harmonic generation of aligned CO<sub>2</sub>," *Phys. Rev. A* **83**, 053409 (2011).
- [35] C. Vozzi, M. Negro, F. Calegari, G. Sansone, M. Nisoli, S. De Silvestri, and S. Stagira, "Generalized molecular orbital tomography," *Nat. Phys.* **7**, 822-826 (2011).
- [36] K. Kato, S. Minemoto, and H. Sakai, "Suppression of high-order-harmonic intensities observed in aligned CO<sub>2</sub> molecules with 1300-nm and 800-nm pulses," *Phys. Rev. A* **84**, 021403(R) (2011).
- [37] A. Rupenyan, P. M. Kraus, J. Schneider, and H. J. Wörner, "Quantum interference and multielectron effects in high-harmonic spectra of polar molecules," *Phys. Rev. A* **87**, 031401(R) (2013).
- [38] A. Rupenyan, P. M. Kraus, J. Schneider, and H. J. Wörner, "High-harmonic spectroscopy of isoelectronic molecules: Wavelength scaling of electronic-structure and multielectron effects," *Phys. Rev. A* **87**, 033409 (2013).
- [39] M. Qin, X. Zhu, Y. Li, Q. Zhang, P. Lan, and P. Lu, "Probing rotational wave-packet dynamics with the structural minimum in high-order harmonic spectra," *Opt. Express* **22**, 6362-6371 (2014).
- [40] H. Yun, K.-M. Lee, J. H. Sung, K. T. Kim, H. T. Kim, and C. H. Nam, "Resolving Multiple Molecular Orbitals Using Two-Dimensional High-Harmonic Spectroscopy," *Phys. Rev. Lett.* **114**, 153901 (2015).
- [41] B. D. Bruner, Z. Mašín, M. Negro, F. Morales, D. Brambila, M. Devetta, D. Faccialà, A. G. Harvey, M. Ivanov, Y. Mairesse, S. Patchkovskii, V. Serbinenko, H. Soifer, S. Stagira, C. Vozzi, N. Dudovich, and O. Smirnova, "Multidimensional high harmonic spectroscopy of polyatomic molecules: detecting sub-cycle laser-driven hole dynamics upon ionization in strong mid-IR laser fields," *Faraday Discuss.* **194**, 369-405 (2016).
- [42] N. Suárez, A. Chacón, J. A. Pérez-Hernández, J. Biegert, M. Lewenstein, and M. F. Ciappina, "High-order-harmonic generation in atomic and molecular systems," *Phys. Rev. A* **95**, 033415 (2017).
- [43] M. Ruberti, P. Decleva, and V. Averbukh, "Multi-channel dynamics in high harmonic generation of aligned CO<sub>2</sub>: ab initio analysis with time-dependent B-spline algebraic diagrammatic construction," *Phys. Chem. Chem. Phys.* **20**, 8311-8325 (2018).
- [44] T. Gorman, T. Scarborough, P. Abanador, F. Mauger,

- D. Kiewewetter, P. Sándor, S. Khatri, K. Lopata, K. J. Schafer, P. Agostini, M. Gaarde, and L. DiMauro, “Probing the interplay between geometric and electronic-structure features via high-harmonic spectroscopy,” *J. Chem. Phys.* **150**, 184308 (2019).
- [45] F. Mauger, P. M. Abanador, T. D. Scarborough, T. T. Gorman, P. Agostini, L. F. DiMauro, K. Lopata, K. J. Schafer, and M. B. Gaarde, “High-harmonic spectroscopy of transient two-center interference calculated with time-dependent density-functional theory,” *Struct. Dyn.* **6**, 044101 (2019).
- [46] R. R. Lucchese and V. McKoy, “Studies of differential and total photoionization cross sections of carbon dioxide,” *Phys. Rev. A* **26**, 1406-1418 (1982).
- [47] C. Jin, A. T. Le, S. F. Zhao, R. R. Lucchese, and C. D. Lin, “Theoretical study of photoelectron angular distributions in single-photon ionization of aligned  $N_2$  and  $CO_2$ ,” *Phys. Rev. A* **81**, 033421 (2010).
- [48] A. T. Le, R. R. Lucchese, M. T. Lee, and C. D. Lin, “Probing Molecular Frame Photoionization via Laser Generated High-Order Harmonics from Aligned Molecules,” *Phys. Rev. Lett.* **102**, 203001 (2009).
- [49] X. M. Tong, Z. X. Zhao, and C. D. Lin, “Theory of molecular tunneling ionization,” *Phys. Rev. A* **66**, 033402 (2002).
- [50] S. F. Zhao, C. Jin, A. T. Le, T. F. Jiang, and C. D. Lin, “Determination of structure parameters in strong-field tunneling ionization theory of molecules,” *Phys. Rev. A* **81**, 033423 (2010).
- [51] C. Jin, A. T. Le, and C. D. Lin, “Medium propagation effects in high-order harmonic generation of Ar and  $N_2$ ,” *Phys. Rev. A* **83**, 023411 (2011).
- [52] X. Zhao, H. Wei, Y. Wu, and C. D. Lin, “Phase-retrieval algorithm for the characterization of broadband single attosecond pulses,” *Phys. Rev. A* **95**, 043407 (2017).
- [53] W.-W. Yu, X. Zhao, H. Wei, S.-J. Wang, and C. D. Lin, “Method for spectral phase retrieval of single attosecond pulses utilizing the autocorrelation of photoelectron streaking spectra,” *Phys. Rev. A* **99**, 033403 (2019).
- [54] V. S. Yakovlev, J. Gagnon, N. Karpowicz, and F. Krausz, “Attosecond Streaking Enables the Measurement of Quantum Phase,” *Phys. Rev. Lett.* **105**, 073001 (2010).
- [55] H. G. Muller, “Reconstruction of attosecond harmonic beating by interference of two-photon transitions,” *Appl. Phys. B: Lasers Opt.* **74**, s17-s21 (2002).
- [56] T. D. Scarborough, T. T. Gorman, F. Mauger, P. Sándor, S. Khatri, M. B. Gaarde, K. J. Schafer, P. Agostini, and L. F. DiMauro, “Full Characterization of a Molecular Cooper Minimum Using High-Harmonic Spectroscopy,” *Appl. Sci.* **8**, 1129 (2018).
- [57] P.-C. Huang, C. Hernández-García, J.-T. Huang, P.-Y. Huang, C.-H. Lu, L. Rego, D. D. Hickstein, J. L. Ellis, A. Jaron-Becker, A. Becker, S.-D. Yang, C. G. Durfee, L. Plaja, H. C. Kapteyn, M. M. Murnane, A. H. Kung, and M.-C. Chen, “Polarization control of isolated high-harmonic pulses,” *Nat. Photon.* **12**, 349-354 (2018).